

Priority Report

EGFR-TKI Resistance Due to *BIM* Polymorphism Can Be Circumvented in Combination with HDAC Inhibition

Takayuki Nakagawa^{1,4}, Shinji Takeuchi¹, Tadaaki Yamada¹, Hiromichi Ebi¹, Takako Sano¹, Shigeki Nanjo¹, Daisuke Ishikawa¹, Mitsuo Sato², Yoshinori Hasegawa², Yoshitaka Sekido³, and Seiji Yano¹

Abstract

BIM (*BCL2L11*) is a BH3-only proapoptotic member of the Bcl-2 protein family. *BIM* upregulation is required for apoptosis induction by EGF receptor (EGFR) tyrosine kinase inhibitors (EGFR-TKI) in *EGFR*-mutant forms of non-small cell lung cancer (NSCLC). Notably, a *BIM* deletion polymorphism occurs naturally in 12.9% of East Asian individuals, impairing the generation of the proapoptotic isoform required for the EGFR-TKIs gefitinib and erlotinib and therefore conferring an inherent drug-resistant phenotype. Indeed, patients with NSCLC, who harbored this host *BIM* polymorphism, exhibited significantly inferior responses to EGFR-TKI treatment than individuals lacking this polymorphism. In an attempt to correct this response defect in the resistant group, we investigated whether the histone deacetylase (HDAC) inhibitor vorinostat could circumvent EGFR-TKI resistance in *EGFR*-mutant NSCLC cell lines that also harbored the *BIM* polymorphism. Consistent with our clinical observations, we found that such cells were much less sensitive to gefitinib-induced apoptosis than *EGFR*-mutant cells, which did not harbor the polymorphism. Notably, vorinostat increased expression in a dose-dependent manner of the proapoptotic BH3 domain-containing isoform of *BIM*, which was sufficient to restore gefitinib death sensitivity in the *EGFR* mutant, EGFR-TKI-resistant cells. In xenograft models, while gefitinib induced marked regression via apoptosis of tumors without the *BIM* polymorphism, its combination with vorinostat was needed to induce marked regression of tumors with the *BIM* polymorphism in the same manner. Together, our results show how HDAC inhibition can epigenetically restore *BIM* function and death sensitivity of EGFR-TKI in cases of *EGFR*-mutant NSCLC where resistance to EGFR-TKI is associated with a common *BIM* polymorphism. *Cancer Res*; 73(8); 2428–34. ©2013 AACR.

Introduction

The EGF receptor (EGFR) tyrosine kinase inhibitors (TKI), gefitinib and erlotinib, have shown marked therapeutic effects against non-small cell lung cancer (NSCLC) with *EGFR*-activating mutations, such as exon 19 deletions and L858R point mutations (1). About 20% to 30% of patients, however, show intrinsic resistance to EGFR-TKIs despite having tumors harboring these *EGFR* mutations. In addition, patients who respond initially later develop acquired resistance to EGFR-TKIs after varying periods of time (2). Among the molecular mechanisms associated with acquired resistance to EGFR-

TKIs are (i) gatekeeper mutations in *EGFR* (i.e., a T790M second mutation), (ii) activation of bypass signaling caused by *Met* amplification or hepatocyte growth factor overexpression, (iii) transformation to small-cell lung cancer, and (iv) epithelial-to-mesenchymal transition (3, 4). Several therapeutic strategies, including new generation EGFR-TKIs and the combination of an EGFR-TKI and a Met-TKI, have been evaluated clinically in patients with *EGFR*-mutant NSCLC who acquired resistance to EGFR-TKIs (2). The mechanisms of intrinsic resistance, however, remain poorly understood.

Recently, a *BIM* deletion polymorphism was reported to be a novel mechanism of intrinsic resistance to EGFR-TKIs (5). *BIM*, also called *BCL2L11*, is a proapoptotic protein and a member of the Bcl-2 family. Gene products (such as *BIM_{EL}*, *BIM_L*, and *BIM_S*) with a BH3 domain, which is essential for apoptosis induction, antagonize antiapoptotic proteins (such as Bcl-2, Bcl-X_L, and Mcl-1) and activate proapoptotic proteins (such as BAX and BAK), thereby inducing apoptosis (6, 7). Activation of BAX and BAK induce cytochrome *c* release into the cytoplasm and result in activation of the caspase cascade (8). *BIM* is pivotal in apoptosis induced by EGFR-TKIs in *EGFR*-mutant NSCLC cells (9). The expression and degradation of *BIM* is regulated mainly by the MEK-ERK pathway (10). The *BIM* deletion polymorphism is relatively common in East Asian populations (12.9%), with 0.5% of individuals being

Authors' Affiliations: ¹Division of Medical Oncology, Cancer Research Institute, Kanazawa University, Kanazawa, Ishikawa; ²Department of Respiratory Medicine, Nagoya University; ³Division of Molecular Oncology, Aichi Cancer Center Research Institute, Nagoya, Aichi; and ⁴Tsukuba Research Laboratories, Eisai Co., Ltd., Ibaraki, Japan

Note: Supplementary data for this article are available at Cancer Research Online (<http://cancerres.aacrjournals.org/>).

Corresponding Author: Seiji Yano, Division of Medical Oncology, Cancer Research Institute, Kanazawa University, 13-1 Takara-machi, Kanazawa, Ishikawa 9200934, Japan. Phone: 81-76-265-2780; Fax: 81-76-234-4524; E-mail: syano@staff.kanazawa-u.ac.jp

doi: 10.1158/0008-5472.CAN-12-3479

©2013 American Association for Cancer Research.

homozygous for this deletion. During the transcription of *BIM*, either exon 3 or exon 4, the latter of which encodes the BH3 domain, is spliced out due to the presence of a stop codon and a polyadenylation signal within exon 3 (11). The *BIM* deletion polymorphism involves the deletion of a 2903 bp fragment in intron 2 and results in the preferential splicing of exon 3 over exon 4, generating a *BIM* isoform that lacks the BH3 domain (5). A retrospective analysis in patients with *EGFR*-mutant NSCLC showed that progression-free survival (PFS) following EGFR-TKI treatment was significantly shorter in patients with the *BIM* polymorphism (6.6 months) than with wild-type *BIM* (11.9 months; ref.5). Another study in patients with *EGFR*-mutant NSCLC treated with EGFR-TKIs also reported that PFS was significantly shorter in patients with BIM-low (4.3 months) than BIM-high (11.3 months) expressing tumors (12), suggesting that reduced expression of BIM with a BH3 domain is associated with an unfavorable response to EGFR-TKIs. To date, however, no therapeutic strategy has yet been developed for patients with *EGFR*-mutant NSCLC with low BIM expression.

Histone deacetylase (HDAC) is an enzyme that regulates chromatin remodeling and is crucial in the epigenetic regulation of various genes (13). Many compounds targeting HDAC have been developed, including vorinostat, an HDAC inhibitor approved by the United States Food and Drug Administration (FDA) for the treatment of patients with cutaneous T-cell lymphoma (14). In mantle cell lymphoma (MCL) cell lines and in cells from patients with MCL, vorinostat induced histone hyperacetylation on promoter regions and consequent transcriptional activation of proapoptotic *BH3*-only genes, including BIM (15). Using *in vitro* and *in vivo* models, we assessed whether the combination of vorinostat and gefitinib restored the expression of BIM protein with a BH3 domain in *EGFR*-mutant NSCLC cells with the *BIM* polymorphism and overcame EGFR-TKI resistance associated with this polymorphism.

Materials and Methods

Cell lines and reagents

The NSCLC cell lines, PC-9, HCC827, and HCC2279, all of which have *EGFR* mutations, were obtained from Immunobiological Laboratories Co., Ltd., the American Type Culture Collection (ATCC), and Dr. John Minna (University of Texas Southwestern Medical Center, Dallas, TX), respectively. PC-3 cells, established from a Japanese female patient with NSCLC and with an exon 19 deletion in *EGFR*, and differing from the prostate cancer cell line PC-3 (ATCC CRL1435), were purchased from Human Science Research Resource Bank (JCRB0077: http://cellbank.nibio.go.jp/~cellbank/cgi-bin/search_res_det.cgi?DB_NUM=1&ID=252 = 1&ID = 252). PC-3 and the other 3 cell lines were maintained in Dulbecco's Modified Eagle's Medium (DMEM) and RPMI-1640 medium, respectively, each supplemented with 10% FBS and antibiotics. All cells were passaged for less than 3 months before renewal from frozen, early-passage stocks. Cells were regularly screened for mycoplasma using a MycoAlert Mycoplasma Detection Kit (Lonza). The cell lines were authenticated at the laboratory of the National Institute of Biomedical Innovation (Osaka, Japan)

by short tandem repeat analysis. Vorinostat and gefitinib were obtained from Selleck Chemicals and AstraZeneca, respectively.

Genotype and expression analysis of *BIM*

Genomic DNA was extracted from cells using DNeasy Blood and Tissue Kits (Qiagen), according to the manufacturer's protocol. Total RNA was extracted from cells using RNeasy PLUS Mini kits (Qiagen). PCR methods were used to detect the *BIM* deletion polymorphism in the samples and the level of expression of *BIM* isoforms (5).

Cell apoptosis

Cells (3×10^3) were seeded into each well of 96-well, white-walled plates, incubated overnight, and treated with the indicated compounds or vehicle [dimethyl sulfoxide (DMSO)] for 48 hours. Cellular apoptosis was analyzed with Caspase-Glo 3/7 assay kits (Promega), which measure caspase-3/7 activity, and PE-Annexin V Apoptosis Detection Kits (BD Biosciences, in accordance with the manufacturers' directions).

Apoptotic cells in tumor xenografts were detected by terminal deoxynucleotidyl transferase-mediated nick end labeling (TUNEL) staining, using the DeadEnd Fluorometric TUNEL system (Promega), according to the manufacturer's protocol.

RNA interference

Duplexed Stealth RNAi (Invitrogen) against *BIM* and Stealth RNAi-negative control low GC Duplex #3 (Invitrogen) were used for RNA interference (RNAi) assays as described (4). The siRNA target sequences were 5'-CAUGAGUUGUGACAAAUC-AACACAA-3' and 5'-UUGUGUUGAUUUGUCACAACUCAUG-3' for BIM #1, and 5'-UGAGUGUGACCGAGAAGGUAGACAA-3' and 5'-UUGUCUACCUUCUGGUCACACUCA-3' for BIM #2.

Western blot analysis

Western blotting was conducted with antibodies against phospho-EGFR (Tyr1068), Akt, phospho-Akt (Ser473), cleaved PARP, cleaved caspase-3, histone H3, acetylated histone H3 (Lys27), BIM, and β -actin (Cell Signaling Technology); and against phospho-Erk1/2 (Thr202/Tyr204), Erk1/2, and EGFR (R&D Systems). Blots were subsequently incubated with horseradish peroxidase-conjugated secondary antibodies specific to mouse or rabbit immunoglobulin G, with signals detected by enhanced chemiluminescence (Pierce Biotechnology).

Subcutaneous xenograft models

Male BALB/cAJcl-nu/nu mice, ages 5 to 6 weeks, were obtained from CLEA Japan Inc and injected subcutaneously into their flanks with cultured tumor cells (5×10^6 cells/0.1 mL/mouse). When tumor volumes reached 100 to 200 mm³, the mice were randomized and treated once daily with gefitinib and/or vorinostat. Each tumor was measured in 2 dimensions, and the volume was calculated using the formula: tumor volume (mm³) = $1/2 \times \text{length (mm)} \times \text{width (mm)}^2$. All animal experiments complied with the Guidelines for the Institute for Experimental Animals, Kanazawa University Advanced Science Research Center (approval No. AP-081088).

Statistical analysis

Between group differences were analyzed by one-way ANOVA. All statistical analyses were conducted using GraphPad Prism Ver. 4.01 (GraphPad Software, Inc.), with $P < 0.05$ considered statistically significant.

Results

EGFR-mutant NSCLC cell lines harboring the *BIM* deletion polymorphism have low susceptibility to gefitinib-induced apoptosis

We first examined the *BIM* deletion polymorphism in *EGFR*-mutant NSCLC cell lines by PCR. PC-9 and HCC827 had wild-type alleles, with a PCR product 4.2 kb in size. Consistent with a previous report (5), HCC2279 cells were heterozygous for the *BIM* deletion polymorphism, with PCR products 4.2 kb (wild-type) and 1.3 kb (2.9 kb deletion polymorphism) in size. Among the 7 additional cell lines with *EGFR* mutations (Supplementary Table S1), PC-3 was heterozygous for the *BIM* deletion polymorphism (Fig. 1A). Western blot analyses reveal that the expression of the proapoptotic BIM protein was markedly lower in PC-3 and HCC2279 than in PC-9 and HCC827 cells. Analysis of *BIM* isoform transcripts showed that cells with the *BIM* polymorphism expressed more exon 3- than exon 4-containing transcripts (Supplementary Fig. S1A and S1B). Treatment with gefitinib enhanced BIM expression, caspase-

3/7 activities, and apoptosis in PC-9 and HCC827 cells much more than in PC-3 and HCC2279 cells (Fig. 1B; Supplementary Fig. S1C, S1D, and S2). Moreover, gefitinib did not increase caspase-3/7 activity in PC-9 and HCC827 cells treated with *BIM* siRNA (Fig. 1C), indicating the crucial role of BIM in apoptosis induction in *EGFR*-mutant NSCLC cells treated with *EGFR*-TKI. These observations clearly showed that *EGFR*-mutant NSCLC cells with the *BIM* deletion polymorphism are much less sensitive to gefitinib, as shown by induction of apoptosis, than cells with wild-type *BIM*.

Vorinostat upregulates *BIM* and efficiently induces apoptosis when combined with gefitinib

Because HDAC inhibition modulates the expression of various genes, including proapoptotic molecules (13), we hypothesized that the HDAC inhibitor, vorinostat, may sensitize *EGFR*-mutant NSCLC cells with the *BIM* polymorphism to gefitinib. In *EGFR*-mutated NSCLC cell lines, including PC-3 and HCC2279 cells, vorinostat dose dependently increased the expression of acetylated histone H3 and BIM with the BH3 domain (Fig. 2A, Supplementary Fig. S3A). We further explored whether the addition of vorinostat to gefitinib induced apoptosis in *EGFR*-mutant NSCLC cells with the *BIM* polymorphism (Fig. 2B and D). In HCC827 and PC-9 cells, which contain only wild-type *BIM*, gefitinib inhibited downstream signaling,

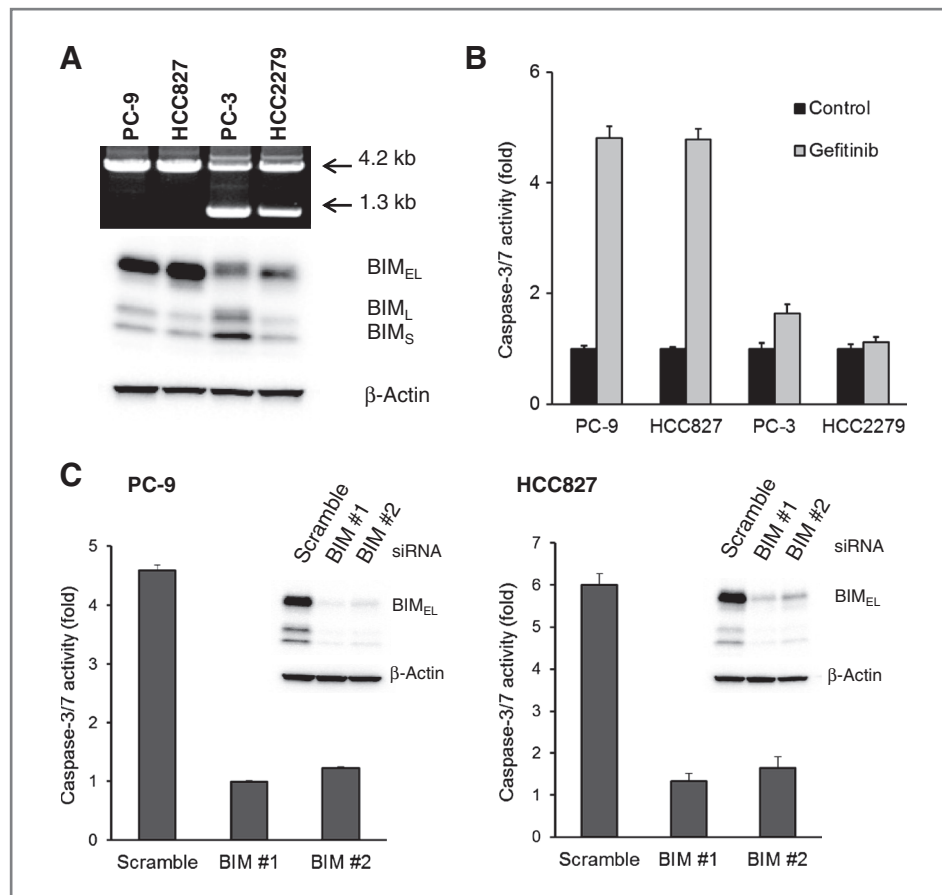


Figure 1. *EGFR*-mutated NSCLC cell lines harboring the *BIM* deletion polymorphism show low susceptibility to gefitinib-induced apoptosis. A, top, PCR products from the 4 *EGFR*-mutated NSCLC cell lines generated by primers flanking the deletion. PCR products 4.2 kb and 1.3 kb in size correspond to the alleles without and with the deletion, respectively, with the presence of both products indicating heterozygosity for the deletion polymorphism. Bottom, the levels of expression of the proteins BIM_{EL}, BIM_L, and BIM_S in each cell line. B, cell lines were treated with gefitinib (1 μ M) or DMSO control for 48 hours, and the activity of caspase-3/7 was measured using Caspase-Glo3/7 assay kits. Each bar represents the mean \pm SD. C, PC-9 (left) and HCC827 (right) cells were transfected with *BIM* or control siRNA for 24 hours before gefitinib (1 μ M) treatment for 48 hours, and the activity of caspase-3/7 was measured as in B. Each bar indicates the mean \pm SD. Lysates were collected and proteins were analyzed by Western blotting.

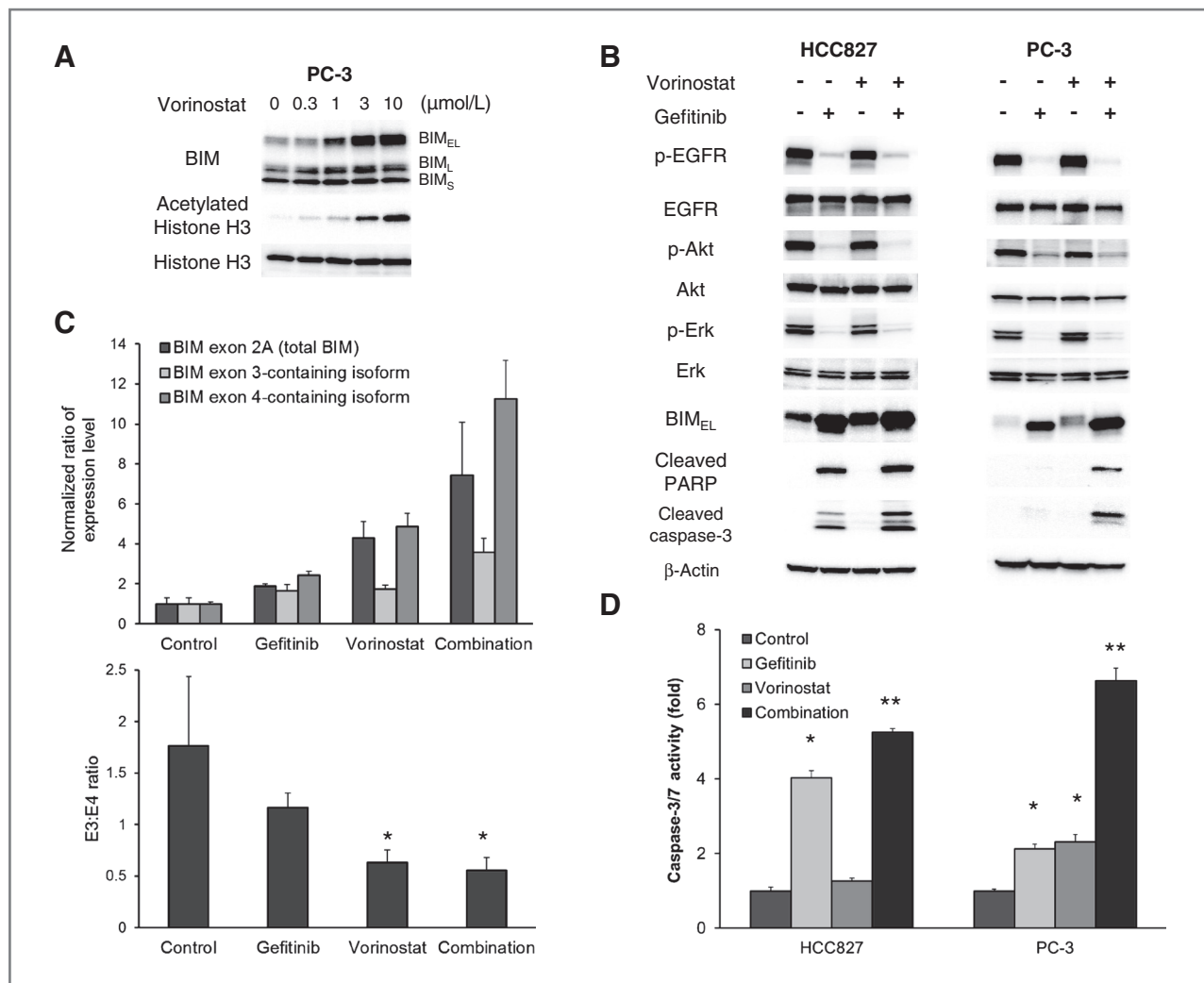


Figure 2. Upregulation of BIM by vorinostat enhances induction of apoptosis in *EGFR*-mutated NSCLC cell line with the *BIM* polymorphism. **A**, PC-3 cells were incubated with serial dilutions of vorinostat for 24 hours. The cell lysates were harvested and the indicated proteins were analyzed by Western blotting. **B**, HCC827 cells (left) and PC-3 cells (right) were incubated with gefitinib (1 μmol/L) and/or vorinostat (3 μmol/L) for 48 hours. The cell lysates were harvested and the indicated proteins were determined by Western blotting. **C**, PC-3 cells were treated with gefitinib (1 μmol/L) and/or vorinostat (3 μmol/L) for 12 hours. The amounts of the various transcripts containing exon 2A, 3, or 4 are expressed as normalized ratios relative to actin (top). Ratio of exon 3-containing transcripts to exon 4-containing transcripts in PC-3 cells after treatment with each compound. *, $P < 0.05$ versus control. Bar indicates the mean \pm SD. **D**, apoptosis was analyzed by measurement of caspase-3/7 activity. *, $P < 0.05$ gefitinib or vorinostat versus control; **, $P < 0.05$ combination versus control and single agents. Bars represent the mean \pm SD.

including the phosphorylation of EGFR, Erk, and Akt, resulting in apoptosis, as shown by the expression of cleaved PARP and cleaved caspase-3. The further addition of vorinostat augmented BIM expression and caspase-3/7 activity. In PC-3 and HCC2279 cells, which contain the *BIM* polymorphism, however, treatment with gefitinib alone induced minimal apoptosis, although the phosphorylation of EGFR, Erk, and Akt was inhibited, whereas the combination of vorinostat and gefitinib markedly increased the expression of BIM, as well as of cleaved PARP and cleaved caspase-3 (Fig. 2B and Supplementary Fig. S3B). This combination also augmented caspase-3/7 activity compared with that of gefitinib or vorinostat alone (Fig. 2D and Supplementary Fig. S3C), but this activation of caspase-3/7 was inhibited by knockdown of *BIM* (Supplementary Fig. S4A and

S4B). Conversely, overexpression of BIM_{EL} itself stimulated caspase-3/7 activities in cells with the *BIM* polymorphism, with these activities further enhanced by gefitinib treatment (Supplementary Fig. S4C and S4D). These results indicate that BIM mediates the activation of caspase-3/7 induced by gefitinib and vorinostat. Analysis of *BIM* transcripts revealed that vorinostat alone induced *BIM* mRNA, which was enhanced by the inclusion of gefitinib. Moreover, vorinostat treatment preferentially induced transcripts containing exon 4 over those containing exon 3 (Fig. 2C). These results indicate that the combination of vorinostat and gefitinib inhibits HDAC and increases the expression of BIM protein with the BH3 domain, thereby sensitizing *EGFR*-mutant NSCLC cells with the *BIM* polymorphism to apoptosis *in vitro*.

Combined treatment with vorinostat with gefitinib shrinks tumors produced by *EGFR*-mutant NSCLC cells with the *BIM* polymorphism

We next determined the *in vivo* efficacy of vorinostat and gefitinib. Gefitinib alone almost completely shrunk xenograft tumors induced by HCC827 cells (Fig. 3A). Although gefitinib monotherapy prevented the enlargement of tumors produced by PC-3 cells, which harbor the *BIM* polymorphism, it did not induce their complete regression, indicating that PC-3 cells remained less susceptible to gefitinib *in vivo*. Under these experimental conditions, vorinostat monotherapy inhibited tumor growth slightly, whereas the combination of vorinostat with gefitinib resulted in marked tumor shrinkage (Fig. 3B). None of the mice treated with these agents showed any macroscopic adverse effects, including loss of body weight (data not shown).

To clarify the mechanisms by which vorinostat and gefitinib act *in vivo*, we assessed tumor-cell apoptosis by TUNEL staining. Gefitinib treatment increased the number of apoptotic

cells in HCC827 tumors but had little effect on PC-3 tumors (Fig. 4A and B), indicating that *EGFR*-mutant NSCLC cells with the *BIM* polymorphism are refractory to gefitinib-induced apoptosis *in vivo* as well as *in vitro*. Importantly, although vorinostat alone had little effect on apoptosis, the combination of vorinostat and gefitinib induced marked apoptosis in PC-3 tumors (Fig. 4A and B). Western blot analyses showed that gefitinib induced cleavage of caspase-3 in HCC827, but not in PC-3, tumors. In PC-3 tumors, treatment with gefitinib or vorinostat had little effect on caspase-3 cleavage, whereas their combination increased BIM expression and the cleavage of caspase-3 (Fig. 4C and D). These findings indicate that the combination of vorinostat and gefitinib increases BIM protein expression and induces tumor-cell apoptosis, thereby shrinking tumors produced by *EGFR*-mutant NSCLC cells with the *BIM* polymorphism.

Discussion

EGFR-mutant NSCLC cells with the *BIM* deletion polymorphism show impaired generation of BIM with the proapoptotic BH3 domain, as well as resistance to *EGFR*-TKI-induced apoptosis (5). We have shown here that treatment of cells with the combination of vorinostat, a HDAC inhibitor, and gefitinib, an *EGFR*-TKI, restored the expression of BIM protein with a BH3 domain (predominantly BIM_{EL}), induced apoptosis, and overcame gefitinib resistance *in vitro* and *in vivo*.

Although vorinostat preferentially induced expression of BIM containing the BH3 domain, its exact mechanisms of action remain unclear. The wild-type allele may be more susceptible to the effects of HDAC inhibition than the deletion allele due to differences in the acetylation status of these alleles. Alternatively, vorinostat may affect the splicing process, resulting in the production of exon 4- rather than exon 3-containing transcripts from the deletion polymorphism allele as HDAC has been found to affect the splicing of RNA (16).

Vorinostat has been shown to induce the expression of several genes other than *BIM* (13). However, we found that BIM was pivotal not only for gefitinib-induced apoptosis but also when combined with vorinostat. Moreover, the combination of vorinostat and gefitinib increased BIM expression and markedly induced apoptosis in PC-3 and HCC2279 cells. Collectively, these findings strongly suggest that vorinostat promotes gefitinib-induced apoptosis in *EGFR*-mutant NSCLC cells with the *BIM* polymorphism, primarily by increasing BIM expression. Several other mechanisms, including inhibition of epigenetic modifications leading to a drug-tolerant state (17) and transition of cancer cells from a resistant mesenchymal state to an E-cadherin-expressing epithelial state (18) may be also involved.

Both the *BIM* polymorphism and *EGFR* mutations are more prevalent in East Asian than in Caucasian populations. Few East Asian patients with *EGFR*-mutant NSCLC show a complete response to *EGFR*-TKIs (1). This incomplete response, including intrinsic resistance, may be due, in part, to low BIM expression associated with the *BIM* polymorphism (6). Our preclinical data indicate that vorinostat increases BIM even in *BIM*-wild type *EGFR*-mutant NSCLC cells. However, a clinical trial with erlotinib and entinostat, an HDAC inhibitor, in

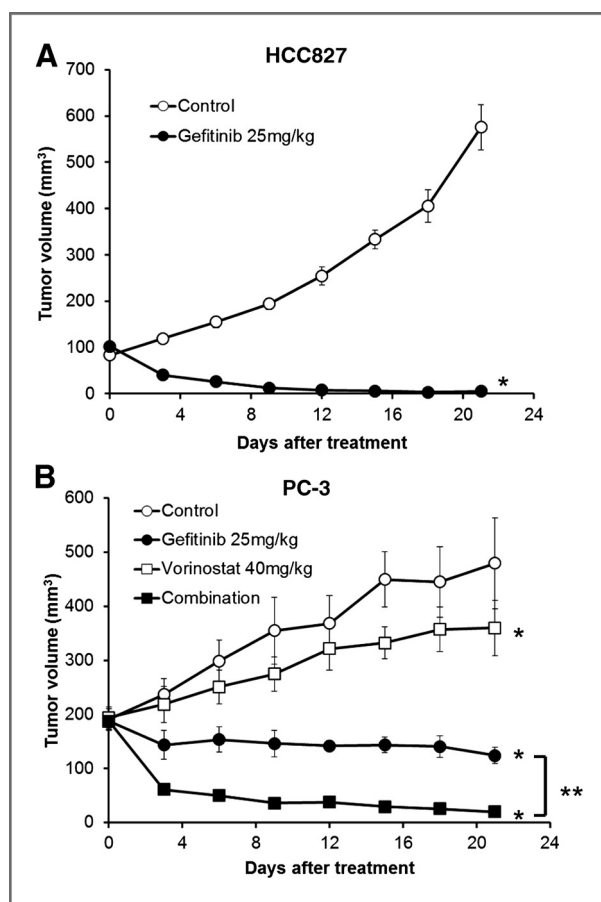


Figure 3. Antitumor activity of gefitinib and/or vorinostat in mouse xenograft models of HCC827 and PC-3 tumors. Nude mice bearing established tumors with HCC827 (A) or PC-3 (B) cells were treated with 25 mg/kg gefitinib and/or 40mg/kg vorinostat once daily for 21 days. Tumor volume was measured using calipers on the indicated days. Mean \pm SE tumor volumes are shown for groups of 4 to 5 mice. *, $P < 0.05$ versus control, **, $P < 0.05$ versus gefitinib by one-way ANOVA.

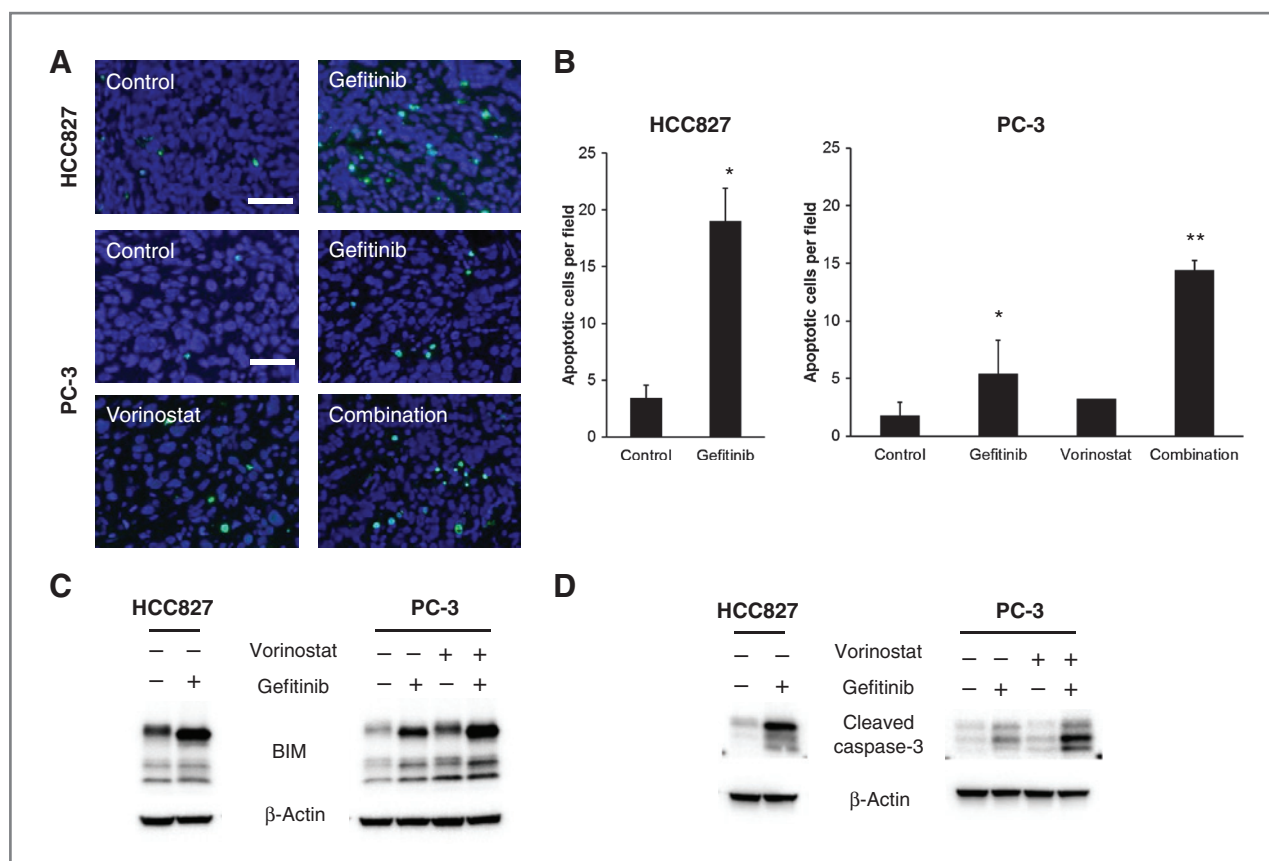


Figure 4. Vorinostat combined with gefitinib increases apoptosis in xenograft tumors with the *BIM* polymorphism. HCC827 and PC-3 xenograft tumors were resected from mice treated with 25 mg/kg gefitinib and/or 40mg/kg vorinostat for 4 days. **A**, analysis of apoptosis by TUNEL staining. Representative fluorescent images are shown. Green fluorescence indicates apoptotic cells. Bar indicates 50 μ m. **B**, quantitation of number of apoptotic cells. *, $P < 0.05$ gefitinib or vorinostat versus control; **, $P < 0.05$ combination versus control and single agents. Bars represent mean \pm SD. **C**, tumors were harvested 8 hours after 2 consecutive treatments with each compound, and the levels of protein in tumor lysates were determined by Western blotting. **D**, tumors were harvested 24 hours after 4 consecutive treatments with each compound. Protein expression levels in the tumor lysates were determined by Western blotting.

unselected patients with NSCLC, more than 65% of whom were Caucasian, failed to show therapeutic benefits (19). These findings suggest that the combination of vorinostat and an EGFR-TKI should be tested in selected patients with NSCLC with *EGFR* mutations and the *BIM* polymorphism.

Resistance to EGFR-TKIs associated with the *BIM* deletion polymorphism may be overcome by treatment with BH3 mimetics, such as ABT-737 (5). Although ABT-737 antagonized antiapoptotic proteins, such as Bcl-2 and Bcl-X_L, it did not antagonize the antiapoptotic protein Mcl-1, which is overexpressed in NSCLC (20), suggesting that the effects of BH3 mimetics may be limited to overcoming EGFR-TKI resistance caused by the *BIM* polymorphism in NSCLC. BH3 mimetics are being evaluated in early-phase clinical trials but are not ready for use in clinical practice. In contrast, vorinostat has been approved by the FDA for the treatment of patients with advanced primary cutaneous T-cell lymphoma (15). Therefore, the combination of gefitinib and vorinostat could easily be tested clinically.

The *BIM* polymorphism can be detected in formalin-fixed paraffin-embedded tumor tissues and peripheral blood (5).

Moreover, a convenient and easy access PCR screening method can detect this polymorphism in circulating DNA from serum (Supplementary Fig. S5A and S5B). As the *BIM* polymorphism is a germline alteration, it can be assayed in serum obtained at any time point. Collectively, our findings illustrate the importance of clinical trials testing the ability of combinations of vorinostat and EGFR-TKIs to overcome EGFR-TKI resistance associated with the *BIM* polymorphism in patients with *EGFR*--mutant NSCLC.

Disclosure of Potential Conflicts of Interest

T. Nakagawa is an employee of Eisai Co., Ltd. for oncology research. Y. Hasegawa received research funding from Chugai Pharmaceutical Co., Ltd., Merck Sharp & Dohme Corp., AstraZeneca, and TAIHO Pharmaceutical Co., Ltd. S. Yano received honoraria from Chugai Pharmaceutical Co., Ltd. and AstraZeneca and received research funding from Chugai Pharmaceutical Co., Ltd., Kyowa Hakko Kirin Co., Ltd., and Eisai Co., Ltd. No potential conflicts of interest were disclosed by the other authors.

Authors' Contributions

Conception and design: T. Nakagawa, S. Takeuchi, S. Nanjo, S. Yano
Development of methodology: T. Nakagawa, S. Takeuchi
Acquisition of data (provided animals, acquired and managed patients, provided facilities, etc.): T. Nakagawa, D. Ishikawa, Y. Hasegawa

Analysis and interpretation of data (e.g., statistical analysis, biostatistics, computational analysis): T. Nakagawa, S. Yano

Writing, review, and/or revision of the manuscript: T. Nakagawa, S. Takeuchi, H. Ebi, M. Sato, Y. Hasegawa, Y. Sekido, S. Yano

Administrative, technical, or material support (i.e., reporting or organizing data, constructing databases): T. Yamada, T. Sano, M. Sato, Y. Sekido
Study supervision: S. Takeuchi, Y. Sekido, S. Yano

Acknowledgments

The authors thank Dr. John Minna (University of Texas Southwestern Medical Center) for the HCC2279 cells.

References

1. Maemondo M, Inoue A, Kobayashi K, Sugawara S, Oizumi S, Isobe H, et al. North-East Japan Study Group. Gefitinib or chemotherapy for non-small-cell lung cancer with mutated EGFR. *N Engl J Med* 2010;362:2380–8.
2. Pao W, Chmielecki J. Rational, biologically based treatment of EGFR-mutant non-small-cell lung cancer. *Nat Rev Cancer* 2010;10:760–74.
3. Sequist LV, Waltman BA, Dias-Santagata D, Digumarthy S, Turke AB, Fidias P, et al. Genotypic and histological evolution of lung cancers acquiring resistance to EGFR inhibitors. *Sci Transl Med* 2011;3:75ra26.
4. Yano S, Wang W, Li Q, Matsumoto K, Sakurama H, Nakamura T, et al. Hepatocyte growth factor induces gefitinib resistance of lung adenocarcinoma with epidermal growth factor receptor-activating mutations. *Cancer Res* 2008;68:9479–87.
5. Ng KP, Hillmer AM, Chuah CT, Juan WC, Ko TK, Teo AS, et al. A common BIM deletion polymorphism mediates intrinsic resistance and inferior responses to tyrosine kinase inhibitors in cancer. *Nat Med* 2012;18:521–8.
6. O'Connor L, Strasser A, O'Reilly LA, Hausmann G, Adams JM, Cory S, et al. Bim: a novel member of the Bcl-2 family that promotes apoptosis. *EMBO J* 1998;17:384–95.
7. Chen L, Willis SN, Wei A, Smith BJ, Fletcher JI, Hinds MG, et al. Differential targeting of prosurvival Bcl-2 proteins by their BH3-only ligands allows complementary apoptotic function. *Mol Cell* 2005;17:393–403.
8. Heath-Engel HM, Shore GC. Regulated targeting of Bax and Bak to intracellular membranes during apoptosis. *Cell Death Differ* 2006;13:1277–80.
9. Costa DB, Halmos B, Kumar A, Schumer ST, Huberman MS, Boggon TJ, et al. BIM mediates EGFR tyrosine kinase inhibitor-induced apoptosis in lung cancers with oncogenic EGFR mutations. *PLoS Med* 2007;4:1669–79.
10. Fukazawa H, Noguchi K, Masumi A, Murakami Y, Uehara Y. BimEL is an important determinant for induction of anoikis sensitivity by mitogen-activated protein/extracellular signal-regulated kinase kinase inhibitors. *Mol Cancer Ther* 2004;3:1281–8.
11. Liu JW, Chandra D, Tang SH, Chopra D, Tang DG. Identification and characterization of Bimgamma, a novel proapoptotic BH3-only splice variant of Bim. *Cancer Res* 2002;62:2976–81.
12. Faber AC, Corcoran RB, Ebi H, Sequist LV, Waltman BA, Chung E, et al. BIM expression in treatment-naive cancers predicts responsiveness to kinase inhibitors. *Cancer Discov* 2011;1:352–65.
13. Bolden JE, Peart MJ, Johnstone RW. Anticancer activities of histone deacetylase inhibitors. *Nat Rev Drug Discov* 2006;5:769–84.
14. Mann BS, Johnson JR, Cohen MH, Justice R, Pazdur R. FDA approval summary: vorinostat for treatment of advanced primary cutaneous T-cell lymphoma. *Oncologist* 2007;12:1247–52.
15. Xargay-Torrent S, Lopez-Guerra M, Saborit-Villarroya I, Rosich L, Campo E, Roue G, et al. Vorinostat-induced apoptosis in mantle cell lymphoma is mediated by acetylation of proapoptotic BH3-only gene promoters. *Clin Cancer Res* 2011;17:3956–68.
16. Delcuve GP, Khan DH, Davie JR. Roles of histone deacetylases in epigenetic regulation: emerging paradigms from studies with inhibitors. *Clin Epigenetics* 2012;4:5.
17. Sharma SV, Lee DY, Li B, Quinlan MP, Takahashi F, Maheswaran S, et al. A chromatin-mediated reversible drug-tolerant state in cancer cell subpopulations. *Cell* 2010;141:69–80.
18. Witta SE, Gemmill RM, Hirsch FR, Coldren CD, Hedman K, Ravdel L, et al. Restoring E-cadherin expression increases sensitivity to epidermal growth factor receptor inhibitors in lung cancer cell lines. *Cancer Res* 2006;66:944–50.
19. Witta SE, Jotte RM, Konduri K, Neubauer MA, Spira AI, Ruxer RL, et al. Randomized phase II trial of erlotinib with and without entinostat in patients with advanced non-small-cell lung cancer who progressed on prior chemotherapy. *J Clin Oncol* 2012;30:2248–55.
20. Cetin Z, Ozbilim G, Erdogan A, Luleci G, Karazum SB. Evaluation of PTEN and Mcl-1 expressions in NSCLC expressing wild-type or mutated EGFR. *Med Oncol* 2010;27:853–60.

Grant Support

This study was supported by Grants-in-Aid for Cancer Research (21390256 to S. Yano; 11019957 to S. Takeuchi), Scientific Research on Innovative Areas "Integrative Research on Cancer Microenvironment Network" (22112010A01 to S. Yano), and Grant-in-Aid for Project for Development of Innovative Research on Cancer Therapeutics (P-Direct) from the Ministry of Education, Culture, Sports, Science, and Technology (MEXT) of Japan.

Received September 3, 2012; revised December 20, 2012; accepted January 19, 2013; published OnlineFirst February 4, 2013.

Cancer Research

The Journal of Cancer Research (1916–1930) | The American Journal of Cancer (1931–1940)

EGFR-TKI Resistance Due to *BIM* Polymorphism Can Be Circumvented in Combination with HDAC Inhibition

Takayuki Nakagawa, Shinji Takeuchi, Tadaaki Yamada, et al.

Cancer Res 2013;73:2428-2434. Published OnlineFirst February 4, 2013.

| | |
|-------------------------------|---|
| Updated version | Access the most recent version of this article at: doi: 10.1158/0008-5472.CAN-12-3479 |
| Supplementary Material | Access the most recent supplemental material at: http://cancerres.aacrjournals.org/content/suppl/2013/02/04/0008-5472.CAN-12-3479.DC1 |

| | |
|------------------------|--|
| Cited articles | This article cites 20 articles, 10 of which you can access for free at: http://cancerres.aacrjournals.org/content/73/8/2428.full#ref-list-1 |
| Citing articles | This article has been cited by 13 HighWire-hosted articles. Access the articles at: http://cancerres.aacrjournals.org/content/73/8/2428.full#related-urls |

| | |
|-----------------------------------|--|
| E-mail alerts | Sign up to receive free email-alerts related to this article or journal. |
| Reprints and Subscriptions | To order reprints of this article or to subscribe to the journal, contact the AACR Publications Department at pubs@aacr.org . |
| Permissions | To request permission to re-use all or part of this article, use this link http://cancerres.aacrjournals.org/content/73/8/2428 . Click on "Request Permissions" which will take you to the Copyright Clearance Center's (CCC) Rightslink site. |